Structural performance of cold-formed lean duplex stainless steel columns

Yuner Huang, Ben Young

Department of Civil Engineering, The University of Hong Kong, Pokfulam Road, Hong Kong, China

Abstract

The structural performance of cold-formed lean duplex stainless steel columns was investigated. A wide range of finite element analysis on square and rectangular hollow sections and other available data, with a total number of 259 specimens, were considered. An accurate finite element model has been created to simulate the pin-ended cold-formed lean duplex stainless steel columns. Extensive parametric study was carried out using the verified finite element model. The column strengths predicted from the parametric study together with the available data are compared with the design strengths calculated from various existing design rules for cold-formed stainless steel structures. It is shown that the existing design rules, except for the ASCE Specification as well as the stub column and full area approach, are conservative. Modifications are proposed for the AS/NZS Standard, EC3 Code, and direct strength method. Reliability analysis was performed to assess the existing and modified design rules. It is also shown that the modified design rules are able to provide a more accurate and reliable predictions for lean duplex stainless steel columns. In this study, it is suggested that the modified design rules in the AS/NZS Standard and the modified direct strength method to be used in designing cold-formed lean duplex stainless steel columns.

Keywords

Cold-formed, design rules, finite element analysis, lean duplex, pin-ended column test, reliability analysis, stainless steel

1 Introduction

Cold-formed stainless steel structures have been increasingly used, due to its high corrosion resistance, aesthetic appearance, ease of construction, and maintenance of structures. The high cost of stainless steel material is one of the main drawbacks for its application in construction projects. In recent years, a relatively new type of lean duplex stainless steel of grade EN 1.4162 (LDX 2101) with high strength and low Nickel content has been developed. The structural and economical advantages of lean duplex stainless steel offer great potential for the use of its material by structural engineers.

Previous researches on the design of column members were mainly focused on austenitic stainless steel grades EN 1.4301 (AISI 304) and EN 1.4401 (AISI 316) as well as ferritic stainless steel grade EN 1.4003 and duplex stainless steel grade EN 1.4462. However, investigation on column members of lean duplex stainless steel is very limited. Young and Hartono [1] conducted tests on austenitic stainless steel grade EN 1.4301 circular hollow section columns, and compared the test results with the existing design rules. It is shown that the current specifications are unconservative in designing compressive members. The design rules proposed by Rasmussen and Hancock [2] and Rasmussen and Rondal [3] are conservative and more reliable than the existing specifications for square hollow section (SHS) and circular hollow section (CHS) columns. Gardner [4] investigated the design of column and beam members of austenitic stainless steel. A new design approach which offers better prediction has been proposed. Young [5] and Young and Lui [6] studied the material properties and structural behaviour of duplex stainless steel grade EN 1.4462 SHS and rectangular hollow section (RHS) columns. It is shown that the current specifications are generally conservative. Theofanous and Gardner [7] carried out experimental and numerical investigations on stub columns and pin-ended columns of lean duplex stainless steel SHS and RHS columns. It is suggested that the class 3 limit ($c/t\varepsilon$) be relaxed from 30.7 to 37.0, and a new effective width equation has been proposed. Huang and Young [8 and 9] conducted a series of stub and pin-ended column tests on lean duplex stainless steel SHS and RHS. It was found that the existing design specifications are generally conservative for column members. A new design approach using stub column properties and full cross-sectional area to calculate compression capacity has been recommended.

The objective of this paper is to study the structural performance of cold-formed lean duplex stainless steel columns. A total number of 259 data, including the numerical results obtained from the parametric study in this paper and the available data, were compared with the existing American Specification [10], Australian/New Zealand Standard [11], European Code [12] as well as the design rules proposed by Theofanous and Gardner [7] based on European Code, direct strength method (DSM), and the stub column and full area approach proposed by Huang and Young [9]. It should be noted that the lean duplex stainless steel is currently not covered by the ASCE [10], AS/NZS [11] and EC3 [12] specifications. Reliability analysis was performed on the existing design rules. Modifications are suggested for the design rules in the AS/NZS, EC3, and DSM. The modified AS/NZS and modified DSM are recommended to be used in designing lean duplex stainless steel columns, due to their accurate and reliable predictions as well as the relatively simple calculation procedure.

2 Finite Element Model for Pin-ended Columns

2.1 General

This section of the paper describes the finite element model by using the program ABAQUS version 6.11 [13] to simulate the cold-formed lean duplex stainless steel pin-ended column tests conducted by Huang and Young [9]. The measured geometry, material properties, residual stresses, initial local and overall geometric imperfections of the test specimens were used in the finite element model (FEM).

2.2 Type of element and Material Modelling

A four-noded doubly curved shell element with reduced integration S4R was used to model the SHS and RHS pin-ended columns. A mesh size of 10 mm × 10 mm (length by width) was adopted in the flat portions of the columns. A finer mesh was used at the corners of the sections to ensure the curvature is accurately modelled. The material modelling used in this study is identical to the FEM as described in Huang and Young [8]. The measured stress-strain curves of flat portions and corners of each section were included in the model. Multi-linear stress-strain curves were used, including the elastic part up to the proportional limit as well as the plastic curves of true stress and logarithmic true plastic strain. The true plastic stress-strain curves converted from flat and corner coupon test results were used in modelling the material properties of the columns.

2.3 Boundary Conditions and Load Application

The pin-ended columns were compressed between pin ends bending about the minor axis. The ends of the columns were simulated by restraining against all degrees of freedom, except for the rotations about the minor axis at two ends and the displacement at the loaded end in the direction of the applied load. The nodes other than the two ends were free to translate and rotate in any directions. The boundary conditions were modelled by two reference points which are coupled with the surfaces of the cross-section at both ends. The effective length (l_e) of the column was assumed to be equal to the length between the two ends of the wedges, which is the sum of specimen length (L), the thicknesses of the two end plates (40 mm) and the heights of the two wedge plates (70 mm), as detailed in Huang and Young [9]. Therefore, the two reference points were located at 55 mm away from each end of the column specimens. The measured eccentricity (e) in each test specimen was also included in the FEM by moving the reference points away from the minor axis. The axial loads were applied by specifying an axial displacement to the nodes at one end of the columns, which is identical to the pin-ended column tests. The loading was applied by a static RIKS step. The nonlinear geometric parameter (*NLGEOM) was used to deal with the large displacement analysis.

2.4 Modelling of Residual Stresses

The residual stresses that exist in cold-formed stainless steel members may have influence on the numerical results. The measured membrane residual stress profile as presented in Huang and Young [8] was incorporated into the FEM of pin-ended column specimen C6L550 [9]. The method of modelling is identical to the stub columns model as described in Huang and Young [8]. The numerical result was compared with column without residual stresses in order to assess the influence of residual stresses in the FEM. The P_{Exp}/P_{FEA} ratio of specimen C6L550 equals to 1.04 for the FEM includes residual stresses, compared with the P_{Exp}/P_{FEA} ratio of 1.05 for the model without residual stresses, where P_{FEA} and P_{Exp} are the numerical column strength predicted by the finite element analysis (FEA) and the test strength, respectively. It is shown that the FEM including residual stresses is only 1% more accurate than that without residual stresses. The comparison of load-axial shortening curves of test and FEA for specimen C6L550 is shown in Fig. 1. It is shown that the effect of residual stresses is negligible at ultimate load of the column. Therefore, the residual stresses were not included in other columns.

2.5 Modelling of Initial Local and Overall Geometric Imperfections

The measured local and overall geometric imperfections of the columns [9] were also included in the FEM. The local and overall buckling modes were superposed on the pin-ended column model. The local and overall buckling modes were separately obtained by carrying out Eigenvalue analyses with large and small depth-to-thickness (D/t) ratio of cross-section, respectively. The BUCKLE procedure available in the ABAQUS library with the load applied within the step was used. The values obtained from the first buckling mode predicted by the ABAQUS Eigenvalue analysis were normalized to 1.0, thus, the buckling mode was then factored by the measured magnitudes of the initial local and overall geometric imperfections of each column.

3 Verification of Finite Element Model

The finite element model was verified with the pin-ended column tests conducted by Huang and Young [9]. The results of the FEA were compared with the test strengths, as shown in Table 1. The mean value of P_{Exp}/P_{FEA} ratio is 1.01 with the coefficient of variation (COV) of 0.059. The value of the P_{Exp}/P_{FEA} ratio ranged from 0.91 to 1.10. The failure modes observed at ultimate load of the experimental specimens that involved material yielding (Y), local buckling (L), flexural buckling (F) and interaction of local and overall flexural buckling (L+F), are identical to those failure modes predicted from the FEA. It should be noted that the yield strength ($A\sigma_{0.2}$) of the column specimen is determined by the 0.2% proof stress (yield stress) at the flat portions multiply by the area of flat portions plus the 0.2% proof stress at the corners multiply by the

area of the corners. In this study, the material yielding (Y) is defined as the ultimate strength greater than the yield strength of the column. Fig. 2 shows the local buckling failure of specimen C5L200 for both the test and FEA. The interaction of local and flexural buckling failure of specimen C6L900 is shown in Fig. 3. The pure flexural buckling failure of specimen C4L1200 is shown in Fig. 4. The failure modes predicted by the FEA agreed well with those observed from the tests. The comparison of load-axial shortening curves obtained from the test and FEA for specimen C1L1200 is shown in Fig. 5. It is observed that the FEM can accurately predict the loading history including the initial stiffness, ultimate strength and axial shortening of the columns.

4 Parametric Study

Finite element analysis on 125 pin-ended columns and 25 stub columns were carried out, using the verified FEM as described earlier and the stub column model reported in Huang and Young [8], respectively. Extensive range of cross-section dimension and column slenderness is designed for the parametric study, including 5 SHS and 20 RHS with 6 different effective lengths in each section. The dimensions of the 25 sections are ranged from 40×40×1 to 420×140×25, among which the aspect ratio (D/B) varies from 1 to 3, and D/t ratio from 8 to 93, where D is the overall depth, B is the overall width, and t is the thickness of the section. The effective length (l_e) of the pin-ended column in the parametric study is equal to the specimen length plus 110 mm, which is the total height of the two pin-ended bearings at both ends. The effective length factor (k) of pin-ended column was taken as 1.0, whereas the effective length of the stub column was assumed to be half of the specimen length. The lengths of the specimens are designed to cover a wide range of column slenderness ratio $\lambda = r_y/l_e$ ranges from around 20 to 100 for each section, where r_y is the radius of gyration.

The material properties obtained from the flat and corner coupon tests of section 70×50×2.5 in Huang and Young [8] are used in the parametric study. The material properties used in the FEM for the flat portions of the cross-sections include the static 0.2% tensile proof stress ($\sigma_{0.2}$) of 613 MPa, static ultimate tensile strength (σ_u) of 738 MPa, Young's modulus (E_o) of 194 GPa, Ramberg-Osgood parameter (n) of 8, and elongation at fracture (ε_f) for a gauge length of 25 mm equal to 44%. The material properties used in FEM for the corners of the cross-sections include $\sigma_{0.2}$ = 844 MPa, σ_u = 995 MPa, E_o = 200 GPa, n = 5, and ε_f = 21%. The average measured local and overall geometric imperfections for the tested specimens reported in Huang and Young [9] are t/11 and L/2165, respectively. Thus, slightly conservative rounded numbers of t/10 and L/2000 were used as the local and overall imperfections in the parametric study, respectively. The effects of residual stress on pin-ended columns are shown to be negligible in this study. Similar finding is reported by Huang and Young [8] for stub columns. Therefore, the profile of residual stresses was not included in the FEM. The specimens are labelled such that the cross-section dimensions and the specimen length could be identified, as shown in Table 2. For example, the label 90×60×1L480 defines the pin-ended column with cross-section (D×B×t) of 90×60×1 in millimeter, and length of 480 mm. The stub column specimens were labelled using two letters "SC" in the prefix of the label. The column strength (P_{FEA}) and failure modes of the parametric study are summarized in Table 2.

5 Reliability Analysis

The reliability of the column design rules is evaluated using reliability analysis. Reliability analysis is detailed in the Commentary of the ASCE Specifications [10]. A target reliability index (β_0) of 2.5 for stainless steel structural members is used as a lower limit in this study. The design rules are considered to be reliable if the reliability index is greater than 2.5. The resistance factors (ϕ_0) of 0.85, 0.90, and 0.91 for concentrically loaded compression members with load combinations of 1.2DL+1.6LL, 1.25DL+1.5LL, and 1.35DL+1.5LL were used in calculating the reliability index (β_0) for ASCE [10], AS/NZS [11], and EC3 [12] respectively, where DL is the dead load and LL is the live load. The load combination of 1.2DL+1.6LL was used for the direct strength method (DSM) in the AISI S100 Specification [14]. The Eq. 6.2-2 in the ASCE Specification [10] was used in calculating the reliability index. The statistical parameters M_m = 1.10, F_m = 1.00, V_m = 0.10 and V_F = 0.05, which are the mean values and coefficients of variation for material properties and fabrication factors for compression members in the commentary of the ASCE Specification were adopted. The mean value (P_m) and coefficient of variation of tests and FEA to design predictions load ratio (V_P) are shown in Tables 3-5. In calculating the reliability index, the correction factor (C_p) as shown in Eq. F1.1-3 of the AISI S100 Specification [14] was used to account for the influence due to a small number of data. For the purpose of direct comparison, a constant resistant factor (ϕ_1) of 0.85 and a load combination of 1.2DL+1.6LL as specified in the ASCE Specifications were used to calculate the reliability index (β_1) for the AS/NZS and EC3 Specifications, and the values of the reliability index are also shown in Table 3 for all columns. The slender and non-slender sections are separately presented in Tables 4 and Table 5.

6 Existing Design Rules & Comparison with Column Strengths

6.1 General

The suitability of existing design rules to lean duplex stainless steel columns are assessed by comparing the test and FEA strengths with the design values. A large data pool of 259 lean duplex stainless steel pin-ended and stub columns that obtained from this study and previous researches is used. The unfactored design strengths (nominal strength) were calculated using six different design rules described in this paper. It should be noted that the lean duplex stainless steel is

not covered in the existing ASCE Specification [10], AS/NZS Standard [11], and EC3 Code [12]. The comparison of the column test strengths with the design strengths is shown in Tables 3 – 5 for all of the specimens, including both slender and non-slender specimens. In this study, slender section is defined when the value of ρ for calculating the effective area in the ASCE [10] is less than unity ($\rho < 1$), meaning that the section is not fully effective. Such method of definition for slender section in the ASCE [10] that is also in the AS/NZS [11] was also applied to the European Code [12], the suggested design rules for EC3 proposed by Theofanous and Gardner [7], direct strength method, and the stub column and full area approach proposed by Huang and Young [9].

6.2 American Specification

In the design rules of ASCE Specification [10], the calculation of design strengths (P_{ASCE}) for columns are detailed in clause 3.4 of the specification for concentrically loaded compression members. The tangent modulus (E_t) is calculated by Eq. B-2 in Appendix B of the ASCE Specification. Iterative process is involved in the calculation. In calculating the effective area (A_e), effective widths were obtained according to clause 2.2.1 of the specification, and the corner areas were considered as fully effective.

Generally speaking, the ASCE Specification provides the most accurate predictions for all columns of slender and non-slender sections, as shown in Table 3. The mean value of the experimental and numerical column strengths (P_u) over the design strengths (P_{ASCE}) ratio P_u/P_{ASCE} is equal to 1.00, the COV equals to 0.106, and the reliability indices (β_o and β_1) equal to 2.59 which are higher than the target value of 2.5. The slender and non-slender sections are separately compared with the design strengths as shown in Tables 4 and 5, respectively. It should be noted that the ASCE Specification is also capable of providing accurate predictions to the slender sections as well as the non-slender sections, with the mean values of P_u/P_{ASCE} ratios equal to 0.98 and 1.00, with the corresponding COV of 0.079 and 0.114 for slender and non-slender sections, respectively. Once again, the reliability indices (β_o and β_1) of 2.61 and 2.58 for slender and non-slender sections, respectively, are higher than the target value. However, the iterative process in calculating the design strengths is more tedious than the other design rules.

6.3 Australian/New Zealand Standard

In AS/NZS Standard [11], the column design strengths ($P_{AS/NZS}$) were calculated using the alternative design method given in clause 3.4.2 of the standard, which is not an iterative process in calculating the design strengths. The calculation of buckling stress (f_n) requires the values of α, β, λ_o and λ_1, as shown in Table 6. It should be noted that the values of lean duplex material are not given in the AS/NZS Standard. Therefore, the values of S31803 (duplex) were used to calculate the buckling stress. The parameters α, β, λ_o and λ_1 are taken as 1.16, 0.13, 0.65 and 0.42, respectively, as shown in Table 6. The calculation of effective areas was based on clause 2.2.1.2 of the standard. Similarly, the corner areas were considered as fully effective.

The AS/NZS Standard provides generally conservative predictions to the lean duplex stainless steel columns, as shown in Table 3 and Fig. 6. The mean value of $P_u/P_{AS/NZS}$ equals to 1.11, with COV of 0.087 for all specimens. It is considered to be reliable with the reliability indices (β_0 and β_0) greater than the target value 2.5. It is observed in Tables 4-5 and Fig. 6 that the predictions of design strengths by AS/NZS Standard are more conservative for the non-slender sections than the slender sections. The mean values of $P_u/P_{AS/NZS}$ equal to 1.04 and 1.14, with COV of 0.097 and 0.072, for slender and non-slender sections respectively. The AS/NZS Standard is considered to be reliable for non-slender sections, with the reliability index (β_0) of 2.82. The reliability index (β_0) for slender sections is equal to 2.38, which is lower than the target value.

6.4 European Code

In the European code, the column design strengths (P_{EC3}) were calculated according to clause 5.4.1 of the EC3 Part 1.4 [12] that referred to clause 6.3.1.1 of the EC3 Part 1.1: General rules and rules for buildings [15], except for the reduction factor (χ) calculated from clause 5.4.2.1 of the EC3 Part 1.4 for uniform members in compression. The imperfection factor α = 0.49 and limiting slenderness $\overline{\lambda}_o$ = 0.4 for hollow sections failed by flexural buckling were used to calculate the reduction factor (χ). Section classification of the specimens according to Table 5.2 of the EC3 Part 1.4 is required in the calculation. Effective areas (A_e) were calculated for class 4 cross-sections. The current class 3 limit ($c/t\varepsilon$) of 30.7 is shown in Fig. 7. According to clause 5.2.3 of the EC3 Part 1.4, the effective widths (b_{eff}) were calculated by EC3 Part 1.5: Plated structural elements [16], except that the reduction factor (ρ) for effective width was calculated by Eq. (1) as follows,

$$\rho = \frac{0.772}{\overline{\lambda}_p} - \frac{0.125}{\overline{\lambda}_p^2} \leq 1 \qquad (1)$$

where $\overline{\lambda}_p$ is the element slenderness. The corner areas were assumed as fully effective.

Tables 3-5 show that the EC3 Code generally provides conservative and reliable predictions for both slender sections and non-slender sections. The mean values of P_u/P_{EC3} equal to 1.15 for all specimens as well as slender sections and

non-slender sections, with COV of 0.078, 0.079, and 0.078, respectively. The reliability indices (β_0 and β_0) are all greater than the target value 2.5, thus, the EC3 Code is considered to be conservative and reliable.

6.5 Suggested Design Rules for European Code

Theofanous and Gardner [7] suggested the class 3 limit ($c/t\varepsilon$) in the Code to be relaxed from 30.7 to 37. In addition, modification is suggested for Eq. (1) to calculate the effective width, where the coefficient 0.125 is replaced by 0.079. The design strengths calculated by the suggested design rules proposed by Theofanous and Gardner [7] are represented by $P_{T\&G}$ in this paper. Compared with the current design rules in EC3 Code, the suggested design rules improves the accuracy of the predictions for slender sections, with the mean value of $P_u/P_{T\&G}$ equals to 1.11 and COV of 0.083, as shown in Table 4. However, the predictions for non-slender sections are similar to the current EC3 Code, with the mean value of $P_u/P_{T\&G}$ of 1.15 and COV of 0.077, as shown in Table 5. For all specimens, it is generally conservative with $P_u/P_{T\&G}$ of 1.14 and COV of 0.080, as shown in Table 3. The suggested design rules are considered to be reliable, as the reliability indices are greater than the target value 2.5.

6.6 Direct Strength Method

The direct strength method (DSM) in this study was based on the clause 1.2.1.1 of Appendix 1 in AISI S100 Specification [14] for the design of cold-formed carbon steel structural members. According to clause 1.2.1.1, the nominal member capacity of a member in compression (P_{DSM}) shall be the minimum of the nominal member capacity of a member in compression for flexural, torsional or flexural-torsional buckling (P_{ne}) and member in compression for local buckling (P_{nl}), as shown in Eqs (2) - (3), where P_y is the nominal yield capacity of the member in compression, λ_c is the non-dimensional slenderness for P_{ne}, λ_l is the non-dimensional slenderness for P_{nl}, and P_{crl} is the critical elastic local column buckling load. It should be noted that distortional buckling will not occur for the RHS and SHS in this study. Therefore, the determination of distortion buckling is not considered. The critical elastic local column buckling load (P_{crl}) of the cross-section was obtained from a rational elastic finite strip buckling analysis [17] with a 5 mm half-wave length interval.

$$P_{ne} = \begin{cases} \left(0.658^{\lambda_c^2}\right)P_y & \text{for } \lambda_c \le 1.5 \\ \left(\dfrac{0.877}{\lambda_c^2}\right)P_y & \text{for } \lambda_c > 1.5 \end{cases} \qquad (2)$$

$$P_{nl} = \begin{cases} P_{ne} & \text{for } \lambda_l \le 0.776 \\ \left[1-0.15\left(\dfrac{P_{crl}}{P_{ne}}\right)^{0.4}\right]\left(\dfrac{P_{crl}}{P_{ne}}\right)^{0.4} P_{ne} & \text{for } \lambda_l > 0.776 \end{cases} \qquad (3)$$

It is observed from Tables 3-5 and Fig. 8 that the direct strength method provides quite conservative and scattered predictions for lean duplex stainless steel columns, especially for non-slender sections. The results are expected as the current direct strength method was developed based on cold-formed carbon steel members instead of stainless steel members. The mean values of P_u/P_{DSM} for all specimens as well as slender sections and non-slender sections equal to 1.25, 1.17, and 1.28, with COV of 0.233, 0.163, and 0.249, respectively. The current DSM is considered to be reliable, as the reliability indices (β_0 and β_0) are all greater than the target value 2.5.

6.7 Stub Column and Full Area Approach

As detailed in Huang and Young [9], it is recommended to use the full cross-section area for all classes of sections, including the slender sections, and the material properties obtained from stub columns. This method is relatively simpler compared to the existing design rules, since the calculation of effective area is not required by simply using full cross-section area regardless of slender or non-slender sections, and the classification of cross-section can be averted as required by the EC3 Code. In the FEA parametric study, the material properties of the pin-ended columns were obtained from the stub columns belong to the same section.

The design strengths P^*_{ASCE}, $P^*_{AS/NZS}$ and P^*_{EC3} were calculated using this design approach for ASCE Specification [10], AS/NZS Standard [11], and EC3 Code [12], respectively, and compared with the test and FEA strengths as shown in Tables 3-5. The test and FEA strengths consist of 188 data, where 150 FEA results obtained from the parametric study as well as 32 pin-ended column tests and 6 stub column tests conducted by Huang and Young [8 and 9]. Generally, the three specifications are capable of providing accurate predictions to the lean duplex stainless steel columns by adopting the stub column material properties and full area approach. The mean values of P_u/P^*_{ASCE}, $P_u/P^*_{AS/NZS}$, and P_u/P^*_{EC3} equal to 0.96, 1.06, and 1.06, with the corresponding COV of 0.096, 0.093, and 0.100 for all specimens, respectively, as shown in Table 3. The mean values are close to unity for both slender and non-slender sections for the three Specifications by adopting this approach. The reliability index (β_0) is 2.5 for ASCE Specification, but slightly smaller than the target value of 2.5 for the

AS/NZS Standard and EC3 Code for all specimens. However, by using the resistance factor (ϕ_1) of 0.85, the reliability index (β_1) is generally larger than the target value for all three specifications, as shown in Tables 3-5.

7 Modified Design Rules & Comparison with Column Strengths

As discussed earlier, the ASCE Specification [10] provides accurate and reliable predictions to the lean duplex stainless steel columns, but the calculation is inconvenient due to the iterative process when compared to the existing design rules. The AS/NZS Standard [11] provides generally conservative predictions, especially to the non-slender sections. The calculating process is relatively simple. The EC3 Code [12] provides conservative and reliable predictions. The suggested design rules for European Code proposed by Theofanous and Gardner [7] slightly improved the accuracy of the slender sections, but still conservative for non-slender sections. By adopting the stub column material properties and full area approach proposed by Huang and Young [9], the ASCE, AS/NZS, and EC3 Specifications are able to provide accurate predictions. However, the stub column properties are not conveniently obtained by designers. The direct strength method predictions are quite conservative and scattered, despite of the relatively simple calculation. In this Section of the paper, modifications are suggested to the current AS/NZS Standard, EC3 Code, and the Direct Strength Method, aiming at accurate and reliable prediction with simple and convenient calculation.

7.1 Modified Australian/New Zealand Standard

Different coefficients of buckling stress (α, β, λ_o, λ_1) are provided for different types of cold-formed stainless steel in the AS/NZS Standard [11]. However, the relatively new material of lean duplex stainless steel type EN 1.4162 is not covered in the current AS/NZS Standard, and it is shown that the coefficients for duplex stainless steel of type EN 1.4462 cannot provide good prediction to the test and FEA specimens. It is proposed that a new set of coefficients of buckling stress α, β, λ_o, λ_1 of 0.86, 0.14, 0.67 and 0.45, respectively, are used for lean duplex stainless steel type EN 1.4162, as shown in Table 6. In determining the column design strengths ($P^{\#}_{AS/NZS}$) using the new set of coefficients of buckling stress, the alternative design method given in clause 3.4.2 of the AS/NZS Standard was used. The comparison of the test strengths with the design strengths by using the new buckling stress coefficients ($P^{\#}_{AS/NZS}$) is summarized in Tables 3-5. It is shown that this design approach is more accurate than the current AS/NZS design rules. The mean values of the $P_u/P^{\#}_{AS/NZS}$ equal to 1.06, 1.01 and 1.08 for all specimens as well as the slender sections and non-slender sections, respectively. It provides a less scattered prediction when considering all specimens and slender sections, with the COV equals to 0.082 and 0.079, respectively. It is also recommended that the resistance factor of 0.85 to be used. Hence, the reliability indices (β_1) are higher than the target value of 2.5 for all specimens as well as the slender sections and non-slender sections.

7.2 Modified European Code

The current design rules in EC3 Code provide conservative predictions to both the slender and non-slender sections of lean duplex stainless steel columns. Therefore, the class 3 limit $c/t\varepsilon$ in the EC3 to determine the occurrence of local buckling for lean duplex stainless steel columns is investigated. In calculating the effective area in the ASCE Specification and AS/NZS Standard, when the value ρ is less than unity ($\rho < 1$), the section is considered to be not fully effective due to the occurrence of local buckling. A total of 57 stub columns is presented in Fig. 7, among which 25 stub columns are defined as slender section ($\rho < 1$). Table 7 shows the 25 slender sections stub columns, where the smallest $c/t\varepsilon$ value of these slender sections is 40. It is shown that the class 3 limit of 40 is more accurate in predicting the occurrence of local buckling, as shown in Fig. 7. Therefore, it is suggested to modify the class 3 limit $c/t\varepsilon$ from 30.7 to 40. In addition to the modification on the class 3 limit, Eq. (1) for the calculation of effective width is also suggested to be modified to Eq. (4), where coefficient 0.125 is replaced by 0.1 only. Furthermore, the imperfection values α and $\overline{\lambda_o}$ of 0.49 and 0.4 are replaced by 0.27 and 0.43, respectively.

$$\rho = \frac{0.772}{\overline{\lambda}_p} - \frac{0.1}{\overline{\lambda}_p^2} \leq 1 \qquad (4)$$

Tables 3 – 5 show that the modified EC3 Code is much more accurate to predict the capacities of the lean duplex stainless steel columns. The mean values of $P_u/P^{\#}_{EC3}$ equal to 1.06, 1.07, 1.06, with the COV of 0.086, 0.086, and 0.090, for all specimens as well as slender and non-slender sections, respectively. The reliability indices (β_0 and β_1) are generally greater than the target value, hence, the modified design rules are reliable.

7.3 Modified Direct Strength Method

The direct strength method (DSM) requires the calculation of a member in compression for flexural, torsional or flexural-torsional buckling (P_{ne}), and member in compression for local buckling (P_{nl}). The nominal member capacity shall be determined by the minimum of P_{ne} and P_{nl} since distortional buckling will not take place for the RHS and SHS in this study. In the modification of DSM, it is suggested that the Eqs (2)-(3) to be modified to Eqs (5)-(6) as follows,

$$P_{ne} = \begin{cases} \left(0.87^{\lambda_c^2}\right) P_y & \text{for } \lambda_c \le 1 \\ \left(\dfrac{0.877}{\lambda_c^2}\right) P_y & \text{for } \lambda_c > 1 \end{cases} \quad (5)$$

$$P_{nl} = \begin{cases} P_{ne} & \text{for } \lambda_l \le 0.769 \\ \left[1 - 0.16\left(\dfrac{P_{crl}}{P_{ne}}\right)^{0.4}\right]\left(\dfrac{P_{crl}}{P_{ne}}\right)^{0.4} P_{ne} & \text{for } \lambda_l > 0.769 \end{cases} \quad (6)$$

The nominal member capacities ($P^{\#}_{DSM}$) determined from the modified DSM are shown in Tables 3-5. The comparison results are also shown in Tables 3-5 and Fig. 9. The mean values of $P_u/P^{\#}_{DSM}$ equal to 1.05, 1.01 and 1.07, with COV of 0.163, 0.105, and 0.177 are compared with the mean values of P_u/P_{DSM} equal to 1.25, 1.17, and 1.28, with COV of 0.233, 0.163, and 0.249 for all specimens as well as slender sections and non-slender sections, respectively. It is shown that the modified DSM provides a much more accurate and less scatter predictions than the current DSM in Eqs (2)-(3). The modified DSM is conservative and reliable, where the reliability indices (β_o and β_1) are greater than the target value of 2.5 for all columns.

8 Conclusions

The pin-ended cold-formed lean duplex stainless steel columns have been investigated. A finite element model was developed and compared well with experimental results. A wide range of parametric study of 150 columns was carried out. The results of parametric study together with 109 available experimental and numerical data of lean duplex stainless steel columns were compared with the design strengths calculated from the current ASCE [10], AS/NZS [11] and EC3 [12] specifications as well as the suggested design rules for EC3 proposed by Theofanous and Gardner [7], the current direct strength method [14], and stub column and full area approach proposed by Huang and Young [9]. It is shown that the design strengths calculated from the AS/NZS Standard, EC3 Code and the suggested design rules [7] are generally conservative, while the predictions by ASCE Specification are more accurate but the calculation procedure is less convenient due to the iterative process in determining the buckling stress. The stub column and full area approach [9] generally improves the accuracy of the predictions. The current direct strength method is also found to be conservative, but with large scattered predictions for the columns investigated in this study, especially for the non-slender sections.

Modifications for AS/NZS Standard, EC3 Code, and direct strength method are proposed in this study. The modified design rules are shown to provide more accurate and reliable predictions for cold-formed lean duplex stainless steel columns. Considering the accuracy, reliability and the simplification of calculation, it is recommended that the modified AS/NZS Standard and the modified direct strength method to be used in designing cold-formed lean duplex stainless steel columns. The two recommended methods are capable of producing reliable limit state designs when calibrated with the resistance factor of 0.85.

Acknowledgement

The research work described in this paper was supported by a grant from The University of Hong Kong under the seed funding program for basic research.

Notation

The following symbols are used in this paper:

A	full area
A_e	effective area
B	overall width of specimen
b_{eff}	effective width in European Code
C_p	correction factor
c	flat width of specimen
D	overall depth of specimen
E_o	initial Young's modulus
E_t	tangent modulus
e	eccentricity or ratio of yield stress to initial Young's modulus
F_m	mean value of fabrication factor
f_n	buckling stress in Australian/New Zealand Standard
f_y	yield stress (0.2% proof stress) in Australian/New Zealand Standard and European Code
k	effective length factor
L	length of specimen
l_e	effective length of specimen
M_m	mean value of material factor
n	Ramberg-Osgood parameter
P_{ASCE}	unfactored design strengths (nominal strength) by American Specification
$P_{AS/NZS}$	unfactored design strengths (nominal strength) by American Specification
P_{crl}	critical elastic local buckling load
P_{DSM}	the nominal member capacity of a member in compression
P_{EC3}	unfactored design strengths by European Code
$P_{T\&G}$	unfactored design strengths calculated by design rules in Theofanous and Gardner [7]
P_{Exp}	experimental ultimate load (test strength)
P_{FEA}	ultimate load calculated from finite element analysis
P_m	mean value of test and finite element to design predictions
P_{ne}	nominal member capacity of a member in compression for flexural, torsional or flexural-torsional buckling
P_{nl}	nominal member capacity of a member in compression for local buckling
P_u	ultimate strength of test or finite element specimens
P_y	the nominal yield capacity of the member in compression
$P^{\#}_{AS/NZS}$	unfactored design strengths calculated using the proposed design rules for Australian/New Zealand Standard
$P^{\#}_{DSM}$	unfactored design strengths calculated using the proposed design rules for direct strength method
$P^{\#}_{EC3}$	unfactored design strengths calculated using the proposed design rules for the European Code
P^{*}_{ASCE}	unfactored design strengths calculated using material properties obtained from stub column tests and full area for American Specification
$P^{*}_{AS/NZS}$	unfactored design strengths calculated using material properties obtained from stub column tests and full area for Australian/New Zealand Standard
P^{*}_{EC3}	unfactored design strengths calculated using material properties obtained from stub column tests and full area for European Code
r_y	radius of gyration about minor axis
t	thickness of specimen
V_F	coefficient of variation of fabrication factor
V_m	coefficient of variation of material factor
V_p	coefficient of variation of test and finite element to design predictions
α	coefficient of buckling stress in Australian/New Zealand Standard or imperfection factor in European Code
β	coefficient of buckling stress in Australian/New Zealand Standard
β_0	reliability index
β_1	reliability index
χ	reduction factor for members in compression in European Code
ε	material factor in European Code
ϕ_0	resistance factor
ϕ_1	resistance factor
λ	slenderness factor in American Specification and Australian/New Zealand Standard
λ_c	non-dimensional slenderness to determine P_{ne}
λ_l	coefficient of buckling stress in Australian/New Zealand Standard or the non-dimensional slenderness to determine P_{nl}
λ_o	coefficient of buckling stress in Australian/New Zealand Standard
$\overline{\lambda}_o$	limiting slenderness in European Code

$\overline{\lambda}_p$ element slenderness in European Code
ε_f tensile strain after fracture based on gauge length of 25 mm
ρ reduction factor in effective width calculation
σ_u static ultimate tensile strength
$\sigma_{0.2}$ static 0.2% tensile proof stress

References

[1] Young B, Hartono W. Compression tests of stainless steel tubular members. J Struct Eng 2002; 128(6): 754-761.

[2] Rasmussen KJR, Hancock GJ. Design of cold-formed stainless steel tubular members. I: Columns. J Struct Eng ASCE 1993; 119(8): 2349-2367.

[3] Rasmussen KJR, Rondal J. Strength curves for metal columns. J Struct Eng ASCE 1997; 123(6): 721-728.

[4] Gardner L. A new approach to structural stainless steel design. Imperial College of Science, Technology and Medicine, London; 2002

[5] Young B. Experimental and numerical investigation of high strength stainless steel structures. J Constr Steel Res 2008; 64(11): 1225-1230.

[6] Young B, Lui WM. Tests of cold-formed high strength stainless steel compression members. Thin-Walled Struct 2006; 44(2): 224-234.

[7] Theofanous M, Gardner L. Testing and numerical modelling of lean duplex stainless steel hollow section columns. Eng Struct 2009; 31(12): 3047-3058.

[8] Huang Y, Young B. Material properties of cold-formed lean duplex stainless steel sections. Thin-walled Struct 2012; 54: 72-81.

[9] Huang Y, Young B. Tests of pin-ended cold-formed lean duplex stainless steel columns. (submitted).

[10] ASCE. Specification for the design of cold-formed stainless steel structural members. SEI/ASCE 8-02; Reston, VA: American Society of Civil Engineers; 2002.

[11] AS/NZS. Cold-formed stainless steel structures. Australian/New Zealand Standard, AS/NZS 4673:2001. Sydney, Australia: Standards Australia; 2001.

[12] EC3. Design of steel structures – Part 1.4: General rules – Supplementary rules for stainless steels. European Committee for Standardization, EN 1993-1-4, Brussels; 2006.

[13] ABAQUS Standard User's Manual. Dassault Systemes Simulia Corp., Version 6.11, USA; 2011

[14] AISI. North American Specification for the design of cold-formed steel structural members. AISI S100-2007, North American Cold-formed Steel Specification, American Iron and Steel Institute, Washington, D.C. ; 2007.

[15] EC3. Design of steel structures – Part 1.1: General rules and rules for buildings. European Committee for Standardization, EN 1993-1-1, Brussels; 2005.

[16] EC3. Design of steel structures – Part 1.5: Plated structural elements. European Committee for Standardization, EN 1993-1-5, Brussels; 2006.

[17] Papangelis JP, Hancock GJ. Computer analysis of thin-walled structural members. Comput Struct 1995; 56(1):157-76.

Table 1 Comparison of Test and FEA Results.

Specimens	Tests		FEA		Comparison
	P_{Exp} (kN)	Failure mode	P_{FEA} (kN)	Failure mode	$\frac{P_{Exp}}{P_{FEA}}$
C1L200	259.2	Y	251.8	Y	1.03
C1L550	154.5	F	155.0	F	1.00
C1L900	85.4	F	89.5	F	0.95
C1L1200	55.3	F	57.2	F	0.97
C1L1550	36.2	F	35.8	F	1.01
C2L200	153.4	L	141.7	L	1.08
C2L550	139.3	L	132.1	L	1.05
C2L900	120.8	F	121.7	F	0.99
C2L1200	92.3	F	98.1	F	0.94
C2L1550	65.4	F	69.0	F	0.95
C3L200	355.3	Y	328.1	Y	1.08
C3L550	302.1	L	322.4	L	0.94
C3L900	242.8	F	220.3	F	1.10
C3L1200	146.1	F	159.0	F	0.92
C3L1550	103.9	F	114.6	F	0.91
C4L200	373.1	Y	354.1	Y	1.05
C4L550	352.8	L	342.6	L	1.03
C4L900	270.7	F	270.1	F	1.00
C4L1200	211.2	F	217.3	F	0.97
C4L1550	148.3	F	159.2	F	0.93
C5L200	370.1	L	367.1	L	1.01
C5L550	372.3	L	346.3	L	1.08
C5L900	335.2	L+F	306.3	L+F	1.09
C5L900R	336.0	L+F	306.3	L+F	1.09
C5L1200	249.0	F	257.7	F	0.97
C5L1200R	252.2	F	257.7	F	0.98
C5L1550	193.7	F	205.2	F	0.94
C6L200	404.1	L	413.2	L	0.98
C6L550	353.2	L	340.1	L	1.04
C6L900	333.5	L+F	308.7	L+F	1.08
C6L1200	284.5	L+F	257.0	L+F	1.10
C6L1550	230.0	L+F	212.0	L+F	1.08
				Mean	1.01
				COV	0.059

Table 2 Summary of Finite Element Results in Parametric Study

Specimens	P_{FEA} (kN)	Failure Mode	Specimens	P_{FEA} (kN)	Failure Mode
SC40×40×1L300	64.3	L	SC160×80×8L620	2322.9	Y
40×40×1L300	64.1	L	160×80×8L620	2135.3	L
40×40×1L625	61.8	L	160×80×8L1265	1703.2	L+F
40×40×1L950	54.8	L+F	160×80×8L1910	1302.1	L+F
40×40×1L1275	35.6	L+F	160×80×8L2555	869.4	L+F
40×40×1L1600	24.2	L+F	160×80×8L3200	580.2	L+F
SC40×40×5L250	569.7	Y	SC160×80×8.6L620	2508.7	Y
40×40×5L300	403.7	Y	160×80×8.6L620	2278.1	L
40×40×5L600	301.9	F	160×80×8.6L1265	1812.6	L+F
40×40×5L900	208.1	F	160×80×8.6L1910	1376.2	L+F
40×40×5L1200	135.9	F	160×80×8.6L2555	905.6	L+F
40×40×5L1500	92.2	F	160×80×8.6L3200	611.3	F
SC80×80×4L600	732.0	L	SC280×110×3L1000	692.6	L
80×80×4L600	711.8	L	280×110×3L1000	663.2	L
80×80×4L1250	571.1	L+F	280×110×3L1750	623.2	L
80×80×4L1900	431.5	L+F	280×110×3L2500	521.5	L+F
80×80×4L2550	279.9	L+F	280×110×3L3250	410.3	L+F
80×80×4L3200	187.7	F	280×110×3L4000	325.5	L+F
SC80×80×4.3L600	805.8	Y	SC280×110×5L880	1558.9	L
80×80×4.3L600	763.8	L	280×110×5L880	1502.5	L
80×80×4.3L1200	624.0	L+F	280×110×5L1660	1342.6	L
80×80×4.3L1800	486.7	F	280×110×5L2440	1168.9	L+F
80×80×4.3L2400	333.4	F	280×110×5L3220	970.6	L+F
80×80×4.3L3000	223.2	F	280×110×5L4000	767.5	L+F
SC80×80×8L600	1559.1	Y	SC280×110×14L850	7094.3	Y
80×80×8L600	1359.3	L+F	280×110×14L960	5954.4	L
80×80×8L1200	1067.8	L+F	280×110×14L1720	4871.0	L+F
80×80×8L1800	788.8	F	280×110×14L2480	3874.9	L+F
80×80×8L2400	516.4	F	280×110×14L3240	2814.4	L+F
80×80×8L3000	347.0	F	280×110×14L4000	1964.7	F
SC90×60×1L480	74.3	L	SC280×110×15L850	7557.8	Y
90×60×1L480	73.8	L	280×110×15L900	6422.1	L
90×60×1L985	68.0	L	280×110×15L1675	5230.5	L+F
90×60×1L1490	58.9	L+F	280×110×15L2450	4117.0	L+F
90×60×1L1995	44.4	L+F	280×110×15L3225	2958.8	F
90×60×1L2500	33.7	L+F	280×110×15L4000	2045.4	F
SC90×60×4.5L460	804.3	Y	SC280×110×20L840	10796.5	Y
90×60×4.5L460	744.2	L	280×110×20L900	8289.1	L
90×60×4.5L970	587.7	L+F	280×110×20L1675	6560.6	L+F
90×60×4.5L1480	437.0	F	280×110×20L2450	5036.8	L+F
90×60×4.5L1990	279.6	F	280×110×20L3225	3478.8	F
90×60×4.5L2500	185.6	F	280×110×20L4000	2369.8	F
SC90×60×4.9L460	892.2	Y	SC390×130×19L1170	12659.0	Y
90×60×4.9L460	814.4	L	390×130×19L1000	10795.2	L
90×60×4.9L970	632.6	L	390×130×19L1750	9497.3	L
90×60×4.9L1480	466.7	F	390×130×19L2500	7742.7	L+F
90×60×4.9L1990	297.3	F	390×130×19L3250	6324.0	L+F
90×60×4.9L2500	197.4	F	390×130×19L4000	4709.9	L+F
SC90×60×6L460	1113.1	Y	SC390×130×21L1170	14202.3	Y
90×60×6L460	985.5	L	390×130×21L1000	11946.8	L
90×60×6L970	753.9	L+F	390×130×21L1750	10326.5	L+F
90×60×6L1480	544.4	F	390×130×21L2500	8376.1	L+F
90×60×6L1990	342.5	F	390×130×21L3250	6776.7	L+F
90×60×6L2500	227.4	F	390×130×21L4000	4990.0	F
SC90×60×8L450	1649.2	Y	SC420×140×21L1260	15181.7	Y
90×60×8L480	1261.7	L	420×140×21L1000	13065.3	L
90×60×8L985	938.7	F	420×140×21L1750	11666.5	L
90×60×8L1490	647.9	F	420×140×21L2500	9639.2	L+F
90×60×8L1995	404.0	F	420×140×21L3250	8055.5	L+F
90×60×8L2500	267.9	F	420×140×21L4000	6272.7	F
SC160×80×2L650	303.0	L	SC420×140×23L1260	16673.9	Y

Specimens	P_{FEA} (kN)	Failure Mode	Specimens	P_{FEA} (kN)	Failure Mode
160×80×2L700	293.9	L	420×140×23L1000	14252.6	L
160×80×2L1400	263.2	L	420×140×23L1750	12613.9	L
160×80×2L2100	199.9	L	420×140×23L2500	10362.1	L+F
160×80×2L2800	149.5	L+F	420×140×23L3250	8603.6	L+F
160×80×2L3500	114.2	L+F	420×140×23L4000	6611.8	F
SC160×80×2.5L650	452.2	L	SC420×140×25L1260	18335.3	Y
160×80×2.5L700	429.3	L	420×140×25L1000	15389.7	L
160×80×2.5L1400	368.2	L+F	420×140×25L1750	13507.3	L
160×80×2.5L2100	289.6	L+F	420×140×25L2500	11049.2	L+F
160×80×2.5L2800	219.6	L+F	420×140×25L3250	9233.4	L+F
160×80×2.5L3500	165.1	L+F	420×140×25L4000	6915.3	F
SC160×80×3L660	586.5	L			
160×80×3L660	568.2	L			
160×80×3L1370	491.5	L+F			
160×80×3L2080	406.0	L+F			
160×80×3L2790	299.4	L+F			
160×80×3L3500	210.7	L+F			

Table 3 Comparison of test and FEA strengths with design strengths for all specimens

	$\frac{P_u}{P_{ASCE}}$	$\frac{P_u}{P^*_{ASCE}}$	$\frac{P_u}{P_{AS/NZS}}$	$\frac{P_u}{P^*_{AS/NZS}}$	$\frac{P_u}{P^\#_{AS/NZS}}$	$\frac{P_u}{P_{EC3}}$	$\frac{P_u}{P^*_{EC3}}$	$\frac{P_u}{P_{T\&G}}$	$\frac{P_u}{P^\#_{EC3}}$	$\frac{P_u}{P_{DSM}}$	$\frac{P_u}{P^\#_{DSM}}$
Number of data	259	188	259	188	259	259	188	259	259	259	259
Mean(P_m)	1.00	0.96	1.11	1.06	1.06	1.15	1.06	1.14	1.06	1.25	1.05
COV(V_p)	0.106	0.096	0.087	0.093	0.082	0.078	0.100	0.080	0.086	0.233	0.163
Resistance factor (ϕ_0)	0.85	0.85	0.90	0.90	0.90	0.91	0.91	0.91	0.91	0.85	0.85
Reliability index (β_0)	2.59	2.50	2.67	2.47	2.50	2.84	2.44	2.79	2.50	2.69	2.52
Resistance factor (ϕ_1)	0.85	0.85	0.85	0.85	0.85	0.85	0.85	0.85	0.85	0.85	0.85
Reliability index (β_1)	2.59	2.50	3.10	2.89	2.92	3.27	2.85	3.21	2.90	2.69	2.52

Note: * Stub column properties and full area approach (Huang and Young, 2012b); # Modified design rules

Table 4 Comparison of test and FEA strengths with design strengths for slender sections

	$\frac{P_u}{P_{ASCE}}$	$\frac{P_u}{P^*_{ASCE}}$	$\frac{P_u}{P_{AS/NZS}}$	$\frac{P_u}{P^*_{AS/NZS}}$	$\frac{P_u}{P^\#_{AS/NZS}}$	$\frac{P_u}{P_{EC3}}$	$\frac{P_u}{P^*_{EC3}}$	$\frac{P_u}{P_{T\&G}}$	$\frac{P_u}{P^\#_{EC3}}$	$\frac{P_u}{P_{DSM}}$	$\frac{P_u}{P^\#_{DSM}}$
Number of data	76	62	74	62	75	76	62	76	76	76	76
Mean(P_m)	0.98	1.00	1.04	1.06	1.01	1.15	1.04	1.11	1.07	1.17	1.01
COV(V_p)	0.079	0.084	0.097	0.106	0.079	0.079	0.101	0.083	0.086	0.163	0.105
Resistance factor (ϕ_0)	0.85	0.85	0.90	0.90	0.90	0.91	0.91	0.91	0.91	0.85	0.85
Reliability index (β_0)	2.61	2.68	2.38	2.42	2.32	2.83	2.35	2.68	2.51	2.88	2.64
Resistance factor (ϕ_1)	0.85	0.85	0.85	0.85	0.85	0.85	0.85	0.85	0.85	0.85	0.85
Reliability index (β_1)	2.61	2.68	2.80	2.83	2.74	3.25	2.76	3.10	2.93	2.88	2.64

Note: * Stub column properties and full area approach (Huang and Young, 2012b); # Modified design rules

Table 5 Comparison of test and FEA strengths with design strengths for non-slender sections

	$\frac{P_u}{P_{ASCE}}$	$\frac{P_u}{P^*_{ASCE}}$	$\frac{P_u}{P_{AS/NZS}}$	$\frac{P_u}{P^*_{AS/NZS}}$	$\frac{P_u}{P^\#_{AS/NZS}}$	$\frac{P_u}{P_{EC3}}$	$\frac{P_u}{P^*_{EC3}}$	$\frac{P_u}{P_{T\&G}}$	$\frac{P_u}{P^\#_{EC3}}$	$\frac{P_u}{P_{DSM}}$	$\frac{P_u}{P^\#_{DSM}}$
Number of data	183	127	185	127	184	183	127	183	183	183	183
Mean(P_m)	1.00	0.94	1.14	1.06	1.08	1.15	1.07	1.15	1.06	1.28	1.07
COV(V_p)	0.114	0.096	0.072	0.086	0.077	0.078	0.098	0.077	0.090	0.249	0.177
Resistance factor (ϕ_0)	0.85	0.85	0.90	0.90	0.90	0.91	0.91	0.91	0.91	0.85	0.85
Reliability index (β_0)	2.58	2.41	2.82	2.50	2.58	2.85	2.50	2.84	2.48	2.67	2.50
Resistance factor (ϕ_1)	0.85	0.85	0.85	0.85	0.85	0.85	0.85	0.85	0.85	0.85	0.85
Reliability index (β_1)	2.58	2.41	3.25	2.92	3.01	3.27	2.90	3.27	2.89	2.67	2.50

Note: * Stub column properties and full area approach (Huang and Young, 2012b); # Modified design rules

Table 6 Existing and proposed coefficients of buckling stress in AS/NZS Standard

Coefficients	α	β	λ_o	λ_l
Existing Coefficients for EN 1.4462 (Duplex)	1.16	0.13	0.65	0.42
Proposed Coefficients for EN 1.4162 (Lean duplex)	0.86	0.14	0.67	0.45

Table 7 **Stub column specimens defined as slender section ($\rho < 1$)**

Source	Specimens	D (mm)	B (mm)	t (mm)	L (mm)	$\frac{c}{t\varepsilon}$
FEA results in this study	SC40×40×1L300	40	40	1.0	300	62.2
	SC90×60×1L480	90	60	1.0	480	146.2
	SC160×80×2L650	160	80	2.0	650	129.4
	SC160×80×2.5L650	160	80	2.5	650	102.5
	SC160×80×3L660	160	80	3.0	660	84.6
	SC280×110×3L1000	280	110	3.0	1000	151.8
	SC280×110×5L880	280	110	5.0	880	89.0
Huang & Young [8]	SC2L150	50.5	50.5	1.49	150	49.9
	SC4L210	70.4	50.8	2.52	210	41.6
	SC5L300	100.1	50.9	2.51	300	62.0
	SC6L450	150.0	50.25	2.46	450	98.1
Theofanous & Gardner [7]	100×100×3.74L400	100	100	3.74	400	40
	100×100×3.09L400	100	100	3.09	400	50
	100×100×2.62L400	100	100	2.62	400	60
	100×100×2.28L400	100	100	2.28	400	70
	100×100×2.02L400	100	100	2.02	400	80
	100×100×1.81L400	100	100	1.81	400	90
	100×100×1.64L400	100	100	1.64	400	100
	200×100×7.48L600	200	100	7.48	600	40
	200×100×6.17L600	200	100	6.17	600	50
	200×100×5.25L600	200	100	5.25	600	60
	200×100×4.57L600	200	100	4.57	600	70
	200×100×4.04L600	200	100	4.04	600	80
	200×100×3.63L600	200	100	3.63	600	90
	200×100×3.29L600	200	100	3.29	600	100

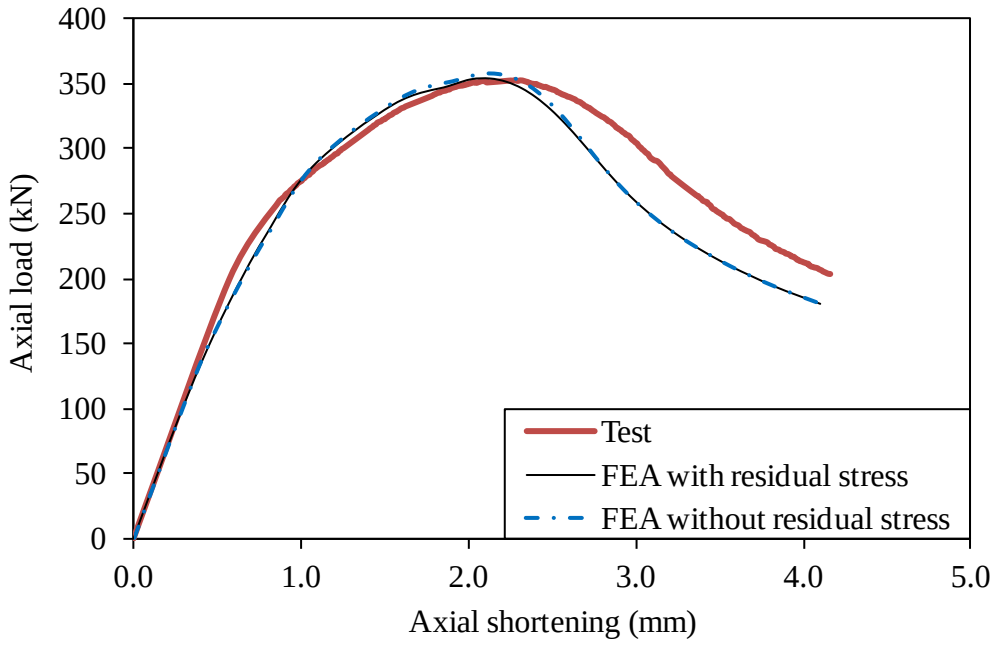

Fig. 1. **Comparison of load-axial shortening curves of test and FEA results for specimen C6L550**

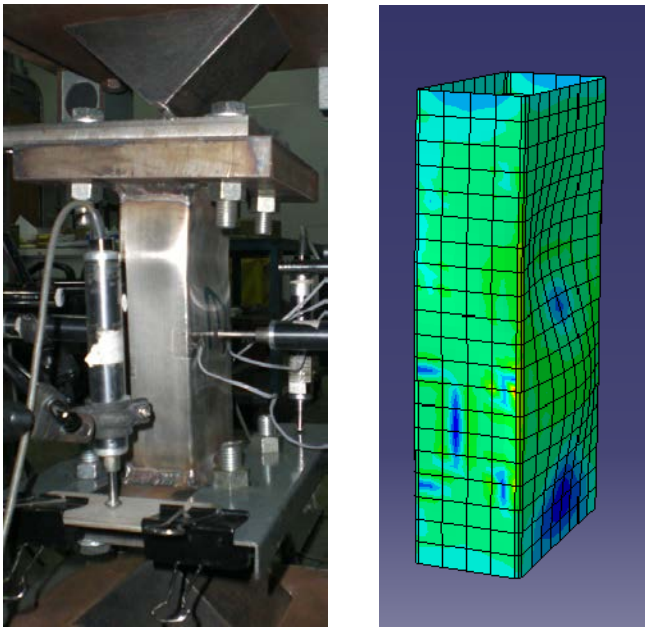

Fig. 2. Local buckling in test and FEA of specimen C5L200

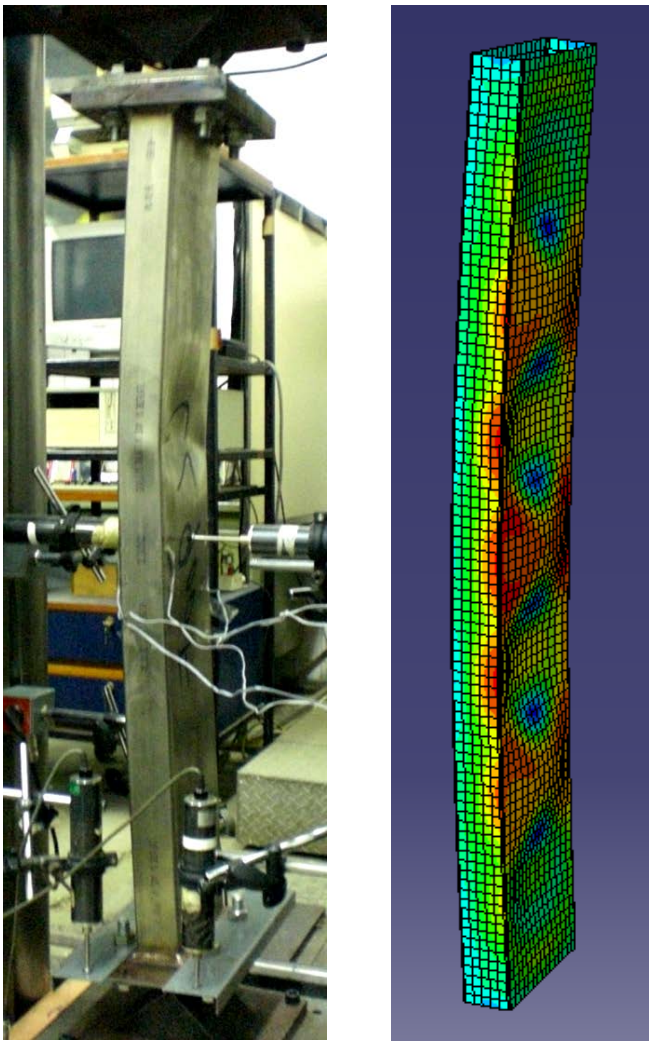

Fig. 3. Interaction of local and flexural buckling in test and FEA of specimen C6L900

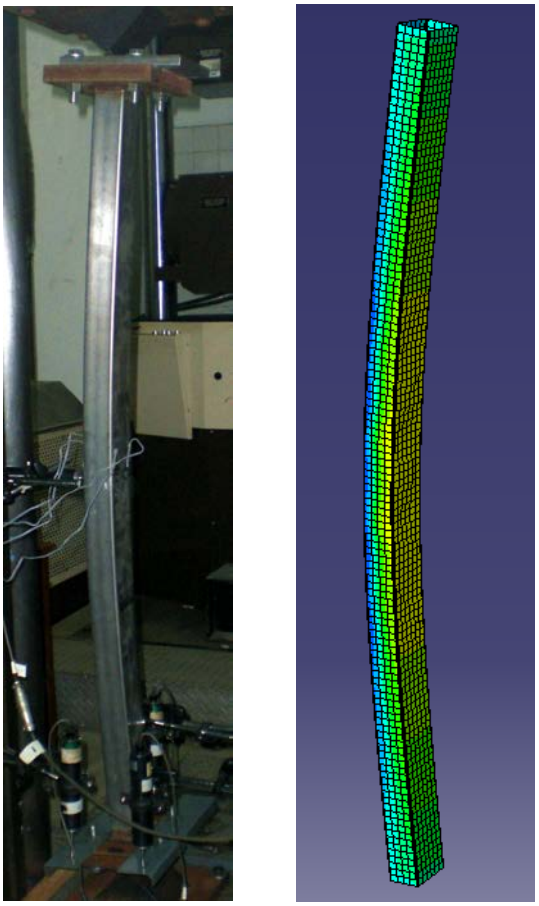

Fig. 4. **Flexural buckling in test and FEA of specimen C4L1200**

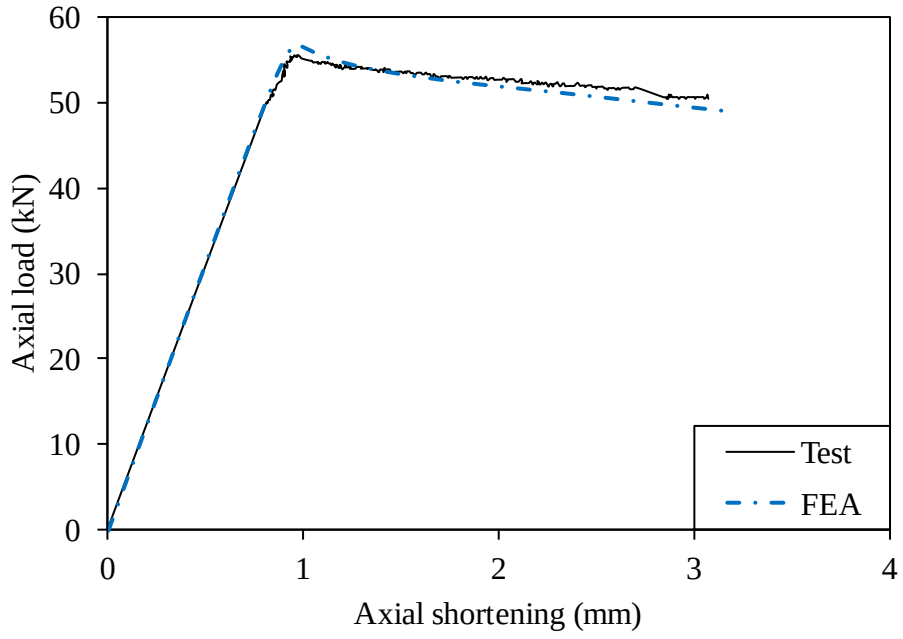

Fig. 5. **Comparison of load-axial shortening curves of test and FEA for specimen C1L1200**

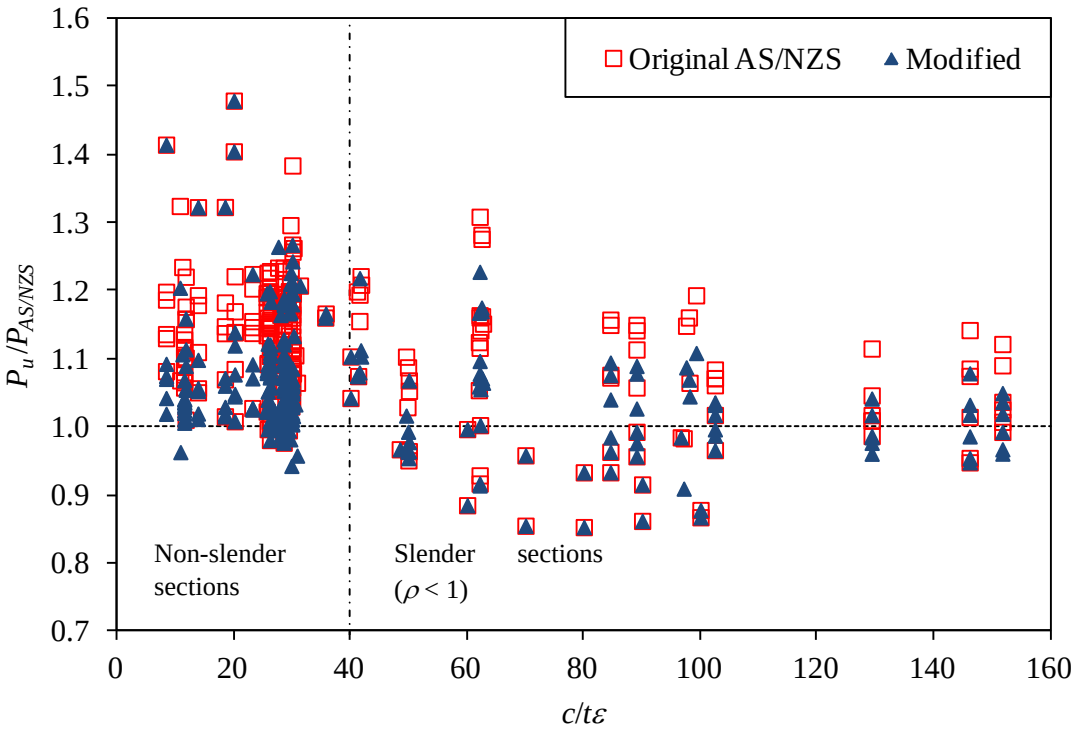

Fig. 6. **Comparison of test and numerical results with design strengths by AS/NZS Standard and modified AS/NZS Standard**

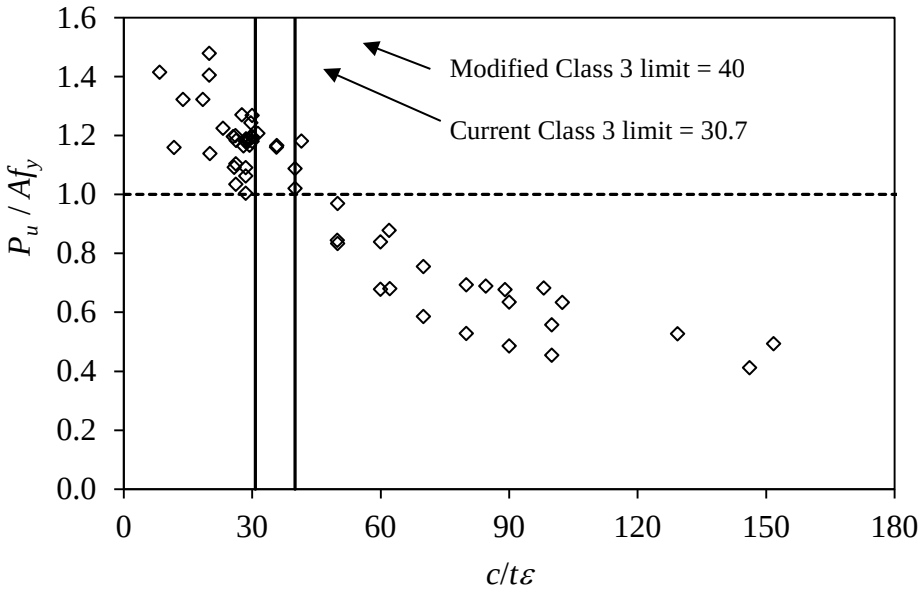

Fig. 7. **Classification of class 3 limit in European Code**

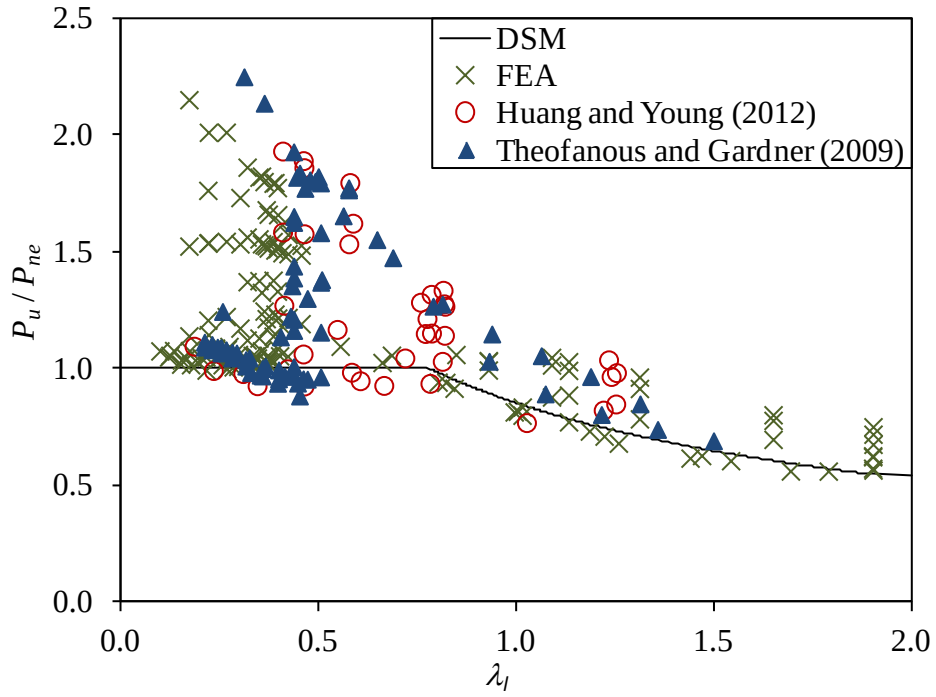

Fig. 8. **Comparison of test and numerical results with design strengths by DSM**

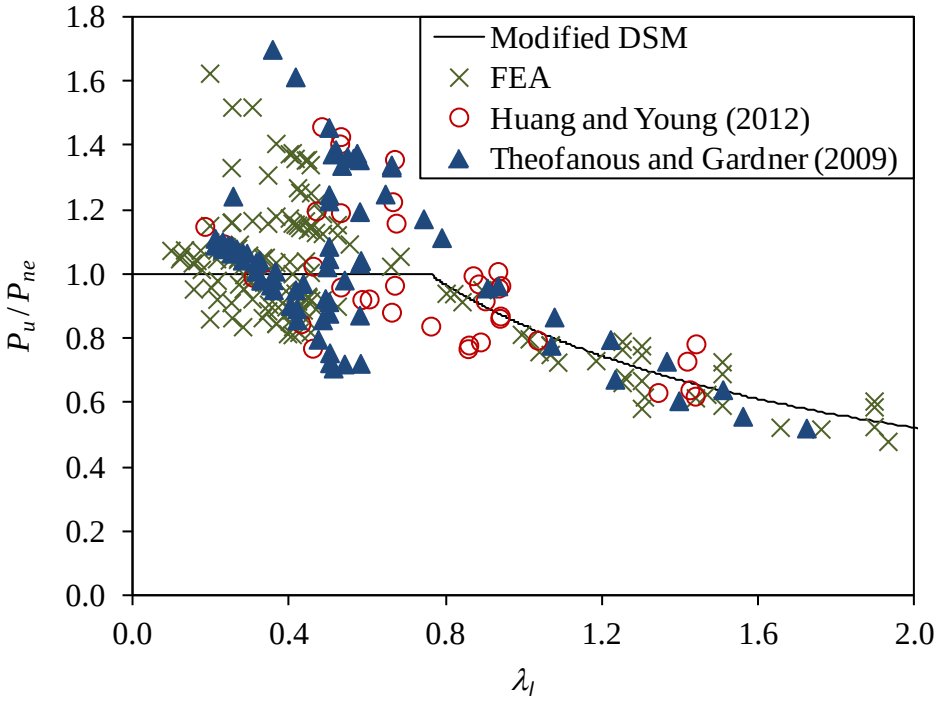

Fig. 9. **Comparison of test and numerical results with design strengths by modified DSM**